Analysis of Monopole Antenna Over a Ground Plane by a Meshless Local Petrov-Galerkin Method

Ramon Dornelas Soares
Elect. Eng. Postgraduate Program
Federal University of Minas Gerais
Av. Antonio Carlos 6627, 31270-901
Belo Horizonte, MG, Brazil
Email: ramon_dornelas@yahoo.com.br

Renato Cardoso Mesquita
Dept. Electrical Engineering
Federal University of Minas Gerais
Av. Antonio Carlos 6627, 31270-901
Belo Horizonte, MG, Brazil
Email: renato@ufmg.br

Fernando Jose da Silva Moreira
Dept. Electronics Engineering
Federal University of Minas Gerais
Av. Antonio Carlos 6627, 31270-901
Belo Horizonte, MG, Brazil
Email: fernandomoreira@ufmg.br

***Abstract*—In this work, two different configurations of a monopole mounted over a ground plane have their input admittance determined by a meshless numerical simulation. The Meshless Local Petrov-Galerkin is used with shape functions generated by Moving Least Squares. Boundary conditions are imposed by a collocation scheme that avoids numerical integrations. The proposed axisymmetric analysis has a simple implementation. The results are in agreement with theoretical data and simulations found in the literature.**

I. Introduction

Monopole antennas have been vastly used due to its simple structure and attractive characteristics. Airborne and ground based systems are some of the most common applications [1]. Several specific applications can also be listed, where the antenna is partially submerged in non-homogeneous environments like oil and water [2], or involved by different mediums as in the coated monopole antenna [3], [4]. Recently, different material have been used in monopole [5] and others studies involving monopole can be found in literature [6], [7].

In [4], the effects of cavities on monopoles are determined using integral equations solved by the method of moments (MoM), which also is used by [5] to validate its proposed model. MoM is known to yield accurate results but with a costly computational effort [2]. The finite element method (FEM) was used in [3], [5], and [6]. FEM simulation produces precise results, but this method needs a mesh with connectivity between the elements, which sometimes demonstrates to be a strong shortcoming. Modal expansion techniques are used in [1], [2] and [7]. In these techniques, a perfectly conductor plane is placed above the antenna and parallel to ground plane, therefore the antenna analyses can be influenced by the waves reflected by it. Precise results are found for particular characteristics of monopole, generally input admittance. This antenna has the main radiation in horizontal direction, minimizing the reflected waves when modal expansion is used.

Meshless methods are a set of powerful numerical techniques providing accurate approximation in mechanic, hydrodynamic, and recently, in electromagnetic area [8]-[16], [18]. These methods can be classified in two main categories: the methods based in strong form and the ones based in weak form. In the Strong form methods, the governing partial differential equations (PDE) are directly discretized using collocations techniques. These methods have a simple algorithm and are computationally efficient. The collocation techniques are generally implemented using radial basis function [8], [9], [10] or smoothed particle hydrodynamics for electromagnetic (SPEM) formulations [11].

In weak form methods, the governing PDE are first transformed in a weak form integral equations generally using the weighted residual method. The weak forms are then used to derive a set of linear equations through a numerical integration process that can be preformed globally or locally in the problem domain [12]. Element free Galerkin (EFG) method uses a global weak form that requires a background mesh to perform numerical integration, so it is not considered a truly meshless method. This method has been successfully applied in the solution of wave scattering problems [12]. The meshless local Petrov-Galerkin (MLPG), used in this work, does not require any mesh and the numerical integration is performed locally in the domain. The weak form is satisfied in a small portion of domain, resulting in sparse matrices and minimizing the computational effort. MLPG has been used to solve wave propagation[13], [14] and [15]. In [16], MLPG method also has been used to solve 3D static problems.

The MLPG analysis proposed in this paper, differently from [16], [13] and [14], uses axisymmetric formulations, as in [3], generating a 2D formulation. Also, it is a weak form method and has advantages when compared to collocation methods in regard to the results precision and numerical stability [17]. The present work extends a previous research [18], where the resonant frequencies and field distribution of axisymmetric cavities were evaluated. Herein, two different configurations of a monopole antenna over a perfectly electric ground plane have their input admittance determined. The monopole 3D perspective is presented in Fig. 1(a) and the axisymmetric monopole model is shown in Fig. 1(b), which presents the antenna length h and its radius r_a. The inner and outer coaxial radii are r_a and r_b, respectively. Figure 1(b) also presents the boundaries of the MPLG model, where $\partial\Omega_c$ denotes the surface of perfectly electric conductor, $\partial\Omega_0$ denotes the symmetry axis ($\rho = 0$), $\partial\Omega_r$ denotes the radiation boundary, and $\partial\Omega_f$ denotes the feed region. The union of all these

978-1-4577-0919-7/12/$26.00 ©2011 IEEE

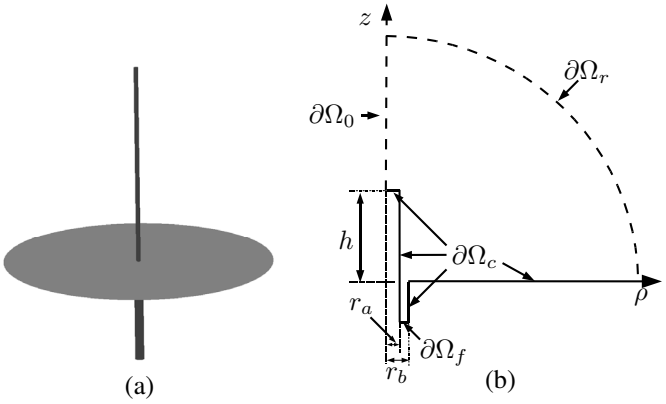

Fig. 1. Monopole over a PEC plane: (a) 3D perspective; (b) 2D monopole model and MLPG boundaries.

boundaries is denoted by $\partial\Omega$.

II. Problem Formulation

The electromagnetic field in a source-free region with relative permittivity ϵ_r and permeability μ_r must satisfy Helmholtz equation, which is given by [19]

$$\nabla \times \left(\frac{1}{\epsilon_r} \nabla \times \vec{H} \right) - k_0^2 \mu_r \vec{H} = 0, \tag{1}$$

where $k_0 = \omega^2 \mu_0 \epsilon_0$ is the free-space wavenumber.

In this work, the material proprieties have axial symmetry, which means that ϵ_r and μ_r do not vary with the azimuthal coordinate ϕ and the antenna excitation is also axisymmetric, ensuring that the electromagnetic field varies only with ρ and z coordinates. Specifically, H_ϕ is the only nonzero magnetic component of the excitation, which means that the magnetic field is given by $\vec{H} = H_\phi(\rho, z)\hat{\phi}$ and that the Helmholtz equation can be expressed in the form

$$\frac{\partial}{\partial \rho}\left[\frac{1}{\rho\epsilon_r}\frac{\partial(\rho H_\phi)}{\partial \rho}\right] + \frac{\partial}{\partial z}\left[\frac{1}{\rho\epsilon_r}\frac{\partial(\rho H_\phi)}{\partial z}\right] + k_0^2 \mu_r H_\phi = 0. \tag{2}$$

Using the weighted residual method with test function $\psi(\rho, z)$ over the problem domain Ω, one obtains the following weak formulation [19]:

$$\oint_{\partial\Omega} \frac{\psi}{\rho\epsilon_r}\frac{\partial(\rho H_\phi)}{\partial n} dl - \iint_\Omega \frac{1}{\rho\epsilon_r} \nabla\psi \cdot \nabla(\rho H_\phi) dA + k_0^2 \iint_\Omega \frac{\mu_r \psi}{\rho}(\rho H_\phi) dA = 0. \tag{3}$$

where Ω is the problem domain in $\rho - z$ semi-plane, in which the infinitesimal area is given by $dA = d\rho dz$.

III. The MLPG Analysis

The MLPG analysis starts by building a set of nodes that are scattered inside the problem domain (interior nodes) and at its boundary $\partial\Omega$ (boundary nodes), as show in Fig. 2. Theses nodes can be scattered in the domain using arbitrary distributions and no connections are set between them. In

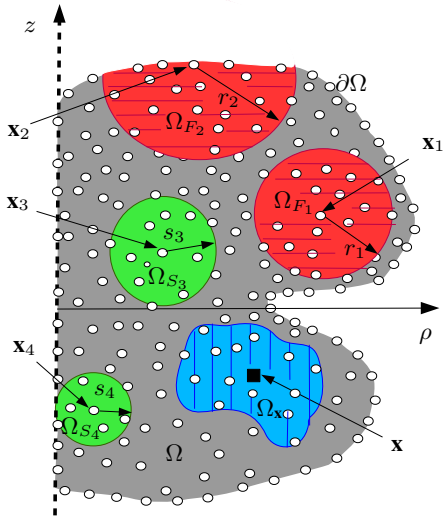

Fig. 2. A computational domain Ω and its boundaries $\partial\Omega$. The horizontal striped regions are the influence domains Ω_{F_1} and Ω_{F_2} of the nodes $\mathbf{x}_1$ and $\mathbf{x}_2$, respectively. The non-striped regions are test domains Ω_{S_3} and Ω_{S_4} of the nodes $\mathbf{x}_3$ and $\mathbf{x}_4$, respectively. The vertical striped region is the support domain Ω_x of a point $\mathbf{x}$.

the proposed study, each node is expressed in cylindrical coordinates as $\mathbf{x}_i = [\rho, z]^T$.

In MLPG method, the weak formulation is satisfied in small local subdomains associated to each node. Therefore, the weak form is integrated over a local quadrature domain, or test domain, which is independent of others node's test domains. This is possible due the Petrov-Galerkin formulation, in which the test function can be chosen to be independent of shape function, φ [20]. The shape functions are built with Moving Least Square (MLS) and they are used to approximate the unknown variables, in (3) given by ρH_ϕ.

Additional techniques are required by MLPG to enforce boundary conditions. In this work, a simple technique known as the meshless collocation scheme is adopted [16] and [17]. In this scheme, the boundary nodes are employed to impose boundary conditions. This strategy is permitted by the Petrov-Galerkin formulation that establishes equations node by node, making possible the MLPG linear system to be built with different sets of equations for interior and boundary nodes [17].

A. MLS Approximation

In MLPG procedure, every node has an associated MLS shape function φ_i, which presents values different from zero only in a small region near the node i. This region is known as node's i influence domains, Ω_{F_i} (see Fig. 2). The local MLS approximation of ρH_ϕ at a point $\mathbf{x}$ is given by

$$u^h(\mathbf{x}) = \sum_{i=1}^{n} \varphi_i(\mathbf{x}) u_i \,, \tag{4}$$

where $i = 1, \ldots, n$ are the nodes whose influence domains include point $\mathbf{x}$ (defined by $\mathbf{x} = [\rho, z]^T$), and u_i are the

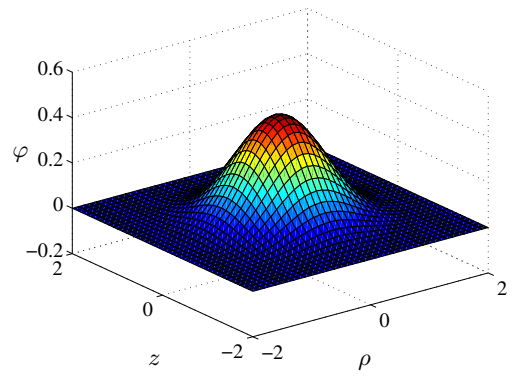

Fig. 3. MLS shape function φ.

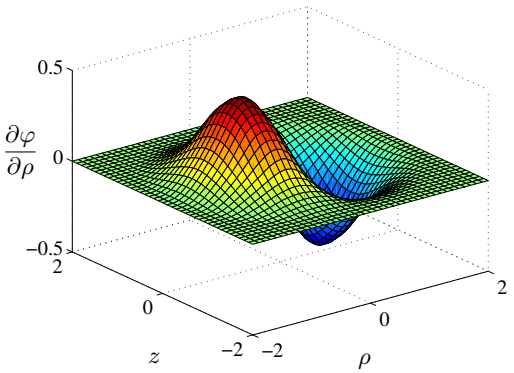

Fig. 4. First derivative of MLS shape function with respect to ρ.

corresponding nodal values. The set of n nodes is known as the support domain $\Omega_{\mathbf{x}}$ (see Fig. 2). The numerical construction of MLS shape function φ_{i} and its derivative (needed to approximate the derivative of unknown variable) involves several matrix manipulations, which are detailed in [17]. Figure 3 shows a MLS shape function for a node located at $\mathbf{x} = [0, 0]^T$ obtained using 25 nodes uniformly spread in Ω. Figure 4 shows an example of the first order shape function derivative with respect to ρ ($\partial\varphi/\partial\rho$).

B. Local Weak Form

In MLPG, the test function ψ_{i} associated to each node has a compact support, which defines the node's test domain $\Omega_{S_{\mathrm{i}}}$ where integrations are evaluated. In this work, the adopted test function is [16], [18]

$$\psi_{\mathrm{i}}(\mathbf{x}) = \begin{cases} \frac{1}{2\pi} \ln\left(\frac{s_{\mathrm{i}}}{|\mathbf{x}-\mathbf{x}_{\mathrm{i}}|}\right) & \text{if } |\mathbf{x}-\mathbf{x}_{\mathrm{i}}| \leq s_{\mathrm{i}}, \\ 0 & \text{if } |\mathbf{x}-\mathbf{x}_{\mathrm{i}}| > s_{\mathrm{i}}, \end{cases} \tag{5}$$

where s_{i} is the radius of the circular domain $\Omega_{S_{\mathrm{i}}}$, chosen such that $\Omega_{S_{\mathrm{i}}}$ does not intersect the global boundary $\partial\Omega$ (see Fig. 2) [16]. $\mathbf{x}_{\mathrm{i}}$ locates node i and $\mathbf{x}$ locates a (tested) point in $\Omega_{S_{\mathrm{i}}}$.

The MLPG local weak form is then obtained from (3) by replacing ψ by ψ_{i} and ρH_ϕ by u^h, where the boundary integral vanishes as $\psi_{\mathrm{i}} = 0$ at the circular boundary of $\Omega_{S_{\mathrm{i}}}$, resulting in:

$$\iint_{\Omega_{S_{\mathrm{i}}}} \frac{\nabla\psi_{\mathrm{i}} \cdot \nabla u^h}{\rho\epsilon_r} dA - k_0^2 \iint_{\Omega_{S_{\mathrm{i}}}} \frac{\mu_r \psi_{\mathrm{i}} u^h}{\rho} dA = 0. \tag{6}$$

This local formulation is versatile; it can be used to analyze a medium with different layers of permittivities or permeabilities (as evaluated in [2], [3] and [4]). In these cases it is necessary to deal with the discontinuity present in the medium, which can be done using the techniques described in [21]. The proposed formulation also can be employed to analyze a monopole placed over a non perfectly electric ground plane. This analysis may be accomplished by using an impedance boundary condition (IBC) when imposing boundary conditions over the metallic surface.

C. Meshless Collocation Scheme

Boundary conditions in $\partial\Omega$ are imposed through the boundary nodes using the meshless collocation scheme that requires no integration [16]. Boundary conditions are expressed in general form as:

$$c(\mathbf{x}_{\mathrm{i}})u^h(\mathbf{x}_{\mathrm{i}}) + d(\mathbf{x}_{\mathrm{i}})\frac{\partial u^h(\mathbf{x}_{\mathrm{i}})}{\partial n} = f(\mathbf{x}_{\mathrm{i}}), \tag{7}$$

where $c = 1$ and $d = 0$ if $\mathbf{x}_{\mathrm{i}}$ is at a Dirichlet boundary or $c = 0$ and $d = 1$ if it is at a Neumann boundary. f is a known imposed value (i.e. $f(\mathbf{x}_{\mathrm{i}}) = 0$ for homogeneous or $f(\mathbf{x}_{\mathrm{i}}) \neq 0$ non-homogeneous case). In the monopole geometry (see Fig. 2), the homogeneous Neumann condition must be imposed along the perfect conducting boundary $\partial\Omega_c$ and the field must satisfy homogeneous Dirichlet condition along the axis of symmetry ($\rho = 0$). In addition, we impose in $\partial\Omega_r$ a first-order radiation boundary condition adapted from [19], which can be expressed by specifying $c = jk\rho^{-1}$, $d = \rho^{-1}$, and $f = 0$ in 7. The excitation at the coaxial waveguide end-wall $\partial\Omega_f$ is imposed by a non-homogeneous Dirichlet condition, which can be imposed making $c = 1$, $d = 0$, and

$$f = \frac{E_0}{\eta} e^{-jk_0 z}, \tag{8}$$

where E_0 is the electric field amplitude imposed at $\partial\Omega_f$ (here $E_0 = 1$ V/m) and η is the intrinsic impedance of the coaxial waveguide dielectric (here, $\eta \approx 120\pi\Omega$).

D. Linear Set of Equations

The numerical solution of the problem is obtained transforming (6) and (7) into a set of linear equations, which results in the following matrix equation:

$$[P]\,[u_{\mathrm{i}}] = [F]\,, \tag{9}$$

where, for interior nodes, the matrix elements are

$$P_{\mathrm{ij}} = \iint_{\Omega_{S_{\mathrm{i}}}} \frac{\nabla\psi_{\mathrm{i}} \cdot \nabla\varphi_{\mathrm{j}}}{\rho\epsilon_r} dA - k_0^2 \iint_{\Omega_{S_{\mathrm{i}}}} \frac{\mu_r \psi_{\mathrm{i}} \varphi_{\mathrm{j}}}{\rho} dA, \tag{10}$$

$$F_{\mathrm{i}} = 0, \tag{11}$$

and, for boundary nodes, they are

$$P_{ij} = c(\mathbf{x}_i)\varphi_j(\mathbf{x}_i) + d(\mathbf{x}_i)\frac{\partial \varphi_j(\mathbf{x}_i)}{\partial n}, \quad (12)$$

$$F_i = f(\mathbf{x}_i). \quad (13)$$

It can be observed that the P matrix is sparse but asymmetric. The non-zero columns in the 'i' line of the P matrix depend upon all nodes 'j' whose influence domains include the node 'i' (if 'i' is a boundary node) or the tested points used to perform numerical integration of Ω_{S_i} (if 'i' is a interior node).

The nodal values u_i can be obtained solving the linear system (9), and afterward they are used to determine ρH_ϕ, at a point $\mathbf{x}$ in the domain, as follows:

$$\rho H_\phi(\mathbf{x}) = \sum_{i=1}^{N} \varphi_i(\mathbf{x}) u_i. \quad (14)$$

IV. Numerical Results

The monopole geometry and main parameters (e.g., length h and radius r_a) are depicted in Fig. 1(b). The inner and outer coaxial radii are r_a and r_b, respectively. Following the investigations conducted in [3] and [2], the monopole is placed over an infinite PEC plane. Figure 1(b) also illustrates the boundaries of the MPLG numerical model. $\partial\Omega_c$ represents PEC surfaces where Neumann conditions ($\partial(\rho H_\phi)/\partial n = 0$) are imposed. $\partial\Omega_0$ represents the symmetry axis where a Dirichlet condition is imposed ($\rho = 0$). $\partial\Omega_r$ represents the hemisphere where a first order radiation boundary condition (RBC) is defined [19]. $\partial\Omega_f$ represents the end-wall of the coaxial waveguide where sources of the TEM mode are impressed with $\rho H_\phi = (E_0/\eta)e^{-jk_0 z}$ and $\eta \approx 120\pi\Omega$.

The input admittances of two different monopole configurations are determined. The first one was previously simulated by FEM in [3], where $r_a = 0.0254\lambda$ and $r_b = 0.0302\lambda$. The second monopole was analyzed by a modal expansion in [2], where $r_a = 0.0095\lambda$ and $r_b = 0.0219\lambda$. For both configurations, $\partial\Omega_f$ are placed 0.1λ below the PEC plane and the admittances are obtained dividing the total electric current at $z = 0$ (ground level) by the interelectrode voltage at the same level. The current is derived from the obtained field ρH_ϕ along the antenna surface and the boundary conditions for a perfect conductor ($\hat{n} \times \vec{H} = \vec{J}_S$). The interelectrode voltage is evaluated by the following field integration:

$$V = \int_{r_a}^{r_b} \vec{E} \cdot \hat{\rho}\, d\rho = j\frac{1}{\omega\epsilon_r\epsilon_0}\int_{r_a}^{r_b} \frac{1}{\rho}\frac{\partial(\rho H_\phi)}{\partial \rho}\, d\rho. \quad (15)$$

Figure 5 shows the input admittance of the first configuration as a function of the monopole length h. Results are in agreement with the FEM simulation of [3] and also with measured data presented in [22]. Figure 6 presents the input admittances of the second antenna configuration, simulated by the present MLPG method and by a modal expansion [2], which are compared with measured data [22].

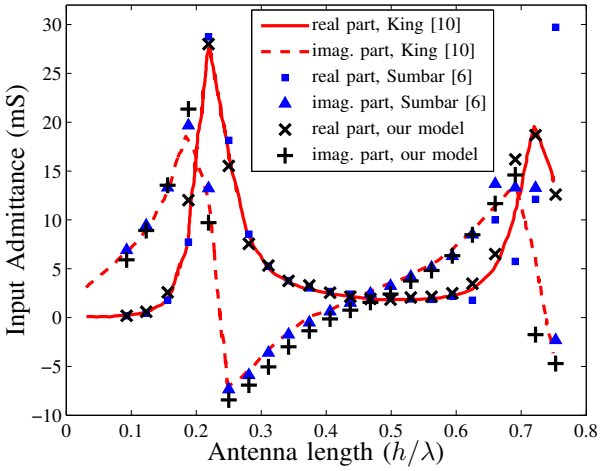

Fig. 5. Input admittance versus antenna length for a monopole over an infinite PEC plane: first antenna configuration [3].

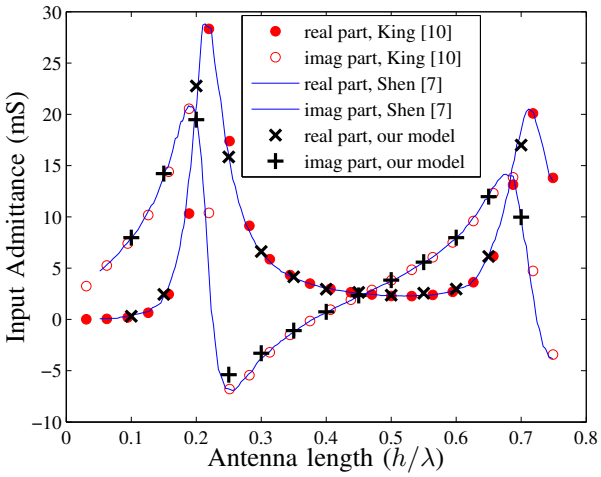

Fig. 6. Input admittance versus antenna length for a monopole over an infinite PEC plane: second antenna configuration [2].

V. Conclusions

This work discussed the numerical analysis of a monopole antenna mounted over an infinite PEC plane by a MLPG method. The axisymmetric weak formulation is simple and versatile, does not require a background mesh (or grid), and produces sparse matrices. The proposed MLPG simulation uses collocation method to impose boundary conditions, simplifying the numerical algorithm. The input admittances of two monopole configurations were analyzed. The results are in agreement with measured data [22] and simulations conducted by other numerical methods [2],[3]. The model is easily adaptable to different axially symmetric geometries and can be used to analyze axisymmetric coated monopoles.

ACKNOWLEDGMENT

Research Project "Numerical Investigation of Coupled Electromagnetic Field Problems", UFMG (Brazil) and McGill University (Canada), CAPES-DFAIT.

REFERENCES

[1] Z. Shen and R. H. MacPhie, "Sleeve monopole on circular ground Plane", *International Journal of Modeling: Electronic Network Devices and Fields*, no. 16, pp. 427-441, 2003.

[2] Z. Shen and R. H. Mac Phie, "Modeling of a Monopole Partially Buried in a Grounded Dielectric Substrate by the modal Expansion Method, *IEEE Trans. Antennas and Propagation*, vol. 44, no. 11, 1996.

[3] E. Sumbar, F. E. Steve, and F. S. Chute, "Implementation of Radiation Boundary Conditions in the Finite Element Analysis of Electromagnetic Wave Propagation", *IEEE Trans. on Microwave Theory and Techniques*, vol. 39, no. 2, 1991.

[4] M. D. Lockard and C. M. Butler, "Effects of Cavities on Monopole Antenna Current Distribution and Decoupling From Mounting Structure", *IEEE Trans. Antennas and Propagation*, vol. 54, no. 8, 2006.

[5] A. Galehdar, P. J. Callus, and K. Ghorbani,"A Novel Method of Conductivity Measurements for Carbon-Fiber Monopole Antenna", *IEEE Trans. Antennas and Propagation*, vol. 59, no. 6, 2011.

[6] K. Y. You, Z. Abbas, K. Khalid, and N. F. Kong,"Improved Formulation for Admittance of Thin and Short Monopole Driving From Coaxial Line Into Dissipative Media", *IEEE Antennas and Wireless Propagation Letters*, vol. 7, 2011.

[7] A. R. Akbarzadeh and Z. Shen,"On the Gap Source Model for Monopole Antennas", *IEEE Antennas and Wireless Propagation Letters*, vol. 7, 2011.

[8] Y. Tanaka and E. Kunisada,"Study on meshless method using RPIM for transient electromagnetic field", *IEEE Trans. Magnetics*, vol. 47, no. 5, pp. 1178-1181, 2011.

[9] Y. Yu and Z.(David) Chen, "A 3-D radial point interpolation method for meshless time-domain modeling", *IEEE Trans. Microwave Theory and Techniques*, vol. 57, no. 8, August 2009.

[10] T. Kaufmann, C. Fumeaus, C. Engstrom, and R. Vahldieck, "Eigenvalue analysis and longtime stability of resonant structures for meshless radial point interpolation method in time domain", *IEEE Trans. Microwave Theory and Techniques*, vol. 58, no. 12, December 2010.

[11] G. Ala, E. Francomano, A. Tortorici, E. Toscano, and F. Viola, "A smoothed particle interpolation scheme for transient electromagnetic simulation", *IEEE Trans. Magnetics*, vol. 42, no. 4, pp. 647-650, 2006.

[12] A. Manzin and O. Bottauscio, "Element-free Galerkin method for the analysis of electromagnetic-wave scattering", *IEEE Trans. Magnetics*, vol. 44, no. 6, pp. 1366-1369, 2008.

[13] B. Correa, E. Silva, A. Fonseca, D. Oliveira, and R. Mesquita, "Meshless local Petrov-Galerkin in solving microwave guide problems". *IEEE Trans. Magnetics*, vol. 47, p. 1526-1529, 2011.

[14] D. S. Junior,"Numerical modelling of electromagnetic wave propagation by meshless local Petrov-Galerkin Formulations", CEMS, vol.50, no.2, pp.97-114, 2009.

[15] W. L. Nicomedes, R. C. Mesquita, and F. J. S. Moreira, "The meshless local Petrov-Galerkin method in two-dimensional electromagnetic wave analysis". *IEEE Trans. on Antennas and Propagation*, accepted for publication, 2012.

[16] W. L. Nicomendes, R. C. Mesquita, and F. J. S. Moreira, "A meshless local Petrov-Galerkin method for three-dimensional scalar problems", *IEEE Trans. Magnetics*, vol. 47, p. 1214-1217, 2011.

[17] G. Liu, *Mesh Free Methods: Moving Beyond the Finite Element Method*, 2nd Ed., CRC Press, 2009.

[18] R. D. Soares, R. C. Mesquita, and F. J. S. Moreira, "Axisymmetric Electromagnetic Resonant Cavities Solution by a meshless Local Petrov-Galerkin Method", The 8th International Conference on Computation in Electromagnetics, Wroclaw, pp 176-177, 2011.

[19] A. Peterson, S. Ray, and R. Mittra, *Computational Methods for Electromagnetics*, IEEE Press, 1998, Sect. 8.8.

[20] G. Liu and Y. Gu, *An introduction to meshfree methods and their programming*, Springer, Berlin, 2005.

[21] Q.Liu, S. Shen, Z. Han, and S. Atluri, "Application of meshless local Petrov-Galerkin (MLPG) to problems with singularities, and material discontinuities, in 3-D elasticity", CMES, vol.4, no5, pp.571-585,2003.

[22] R. King, *Tables of Antenna Characteristics*, IFI/Plenum, NY, 1971.